Electronic Supplementary Material (ESI) for Lab on a Chip.

Supplemental Information

Title: Optimized double emulsion flow cytometry with high-throughput single droplet isolation †

Authors: Kara K. Brower[a,b], Catherine Carswell-Crumpton[c], Sandy Klemm[d], Bianca Cruz[e], Gaeun Kim[a], Suzanne G.K. Calhoun[f], Lisa Nichols[c], and Polly M. Fordyce[a,b,d,g,‡]

Affiliations:
[a]Department of Bioengineering, Stanford University, Stanford, California, USA
[b]Chem-H Institute, Stanford University, Stanford, California, USA
[c]Center for Molecular and Genetic Medicine, Stanford University, Stanford, California, USA
[d]Department of Genetics, Stanford University, Stanford, California, USA
[e]Department of Physics, California State Polytechnic Institute, Pomona, CA, USA
[f]Department of Chemical Engineering, Stanford University, Stanford, California, USA
[g]Chan-Zuckerberg Biohub, San Francisco, CA, USA

Extended Materials and Methods

1. Flow Cytometry Preparation of Double Emulsions

Prior to FACS, DEs were diluted 1:5 in FACS diluent buffer (1% Tween-20) in a 12 x 75 round bottom FACS tube (BD). For a typical run, 100 µL of DEs from the DE pellet at the bottom of the collection vessel (***e.g.*** 1.5 mL Eppendorf) were gently aspirated with a P200 pipette prior to dilution. All DEs were osmotically matched to their suspension media (the outer aqueous sheath high-surfactant mix containing 2% Pluronix F68 (Sigma), **Table 1**) to prevent DE expansion or shrinkage. To process smaller absolute amounts of DE droplets (<100 µL pellets), we recommend supplementing the remaining volume with the outer aqueous sheath high-surfactant mix before dilution in the FACS diluent buffer to increase droplet stabilization during sample loading and FACS injection into the sample line.

Suggestions for Preparation of Double Emulsions for FACS:

- Always use at least 50 µL of droplets from the droplet pellet, if possible, as too few droplets will require sample pausing, manual agitation, and reloading.
- Before loading droplets into the FACS machine, gently swirl or flick the FACS 12 x 75 mm tube, but never vortex. Droplet should be gently resuspended from the white pellet to create a cloudy mixture but vortexing may induce too much shear and result in droplet breakage.
- Manual resuspension may be required during the run, especially in the SH800. If event rate drops below 50 eps after initial gate structuring, pause and resuspend the droplets by gently swirling the sample. Sample line re-positioning to the bottom of the FACS tube can also significantly decrease the need for resuspension.
- Density matching agents (***e.g.*** OptiPrep, xanthan gum, or PEG) may be used but can change typical FSC vs. SSC profiles; the SH800 does not have optionality for an added ND filter and droplet populations may not appear on-scale using these additives. Manual resuspension performs more robustly and reliably for high sort recovery in our hands and is strongly recommended.
- Optically dense samples (e.g., greater than 150 µL of droplets loaded per 500 uL) may result in decreased droplet singlet rates and droplet breakage. Droplets are deformable and can pack in sample loops and nozzles; too many droplets run at once can collide and result in breakage. To process large numbers of droplets, we recommend pausing and continuing to add sample during the run rather beginning with dense samples. The time required for droplet addition is minimal.

2. Droplet Delay Large-Particle Manual Calibration

Before each run, droplet delay times were calibrated using instrument software for the SH800 (Sony) and Aria II (BD) using flow calibration beads (Automatic Setup Beads, Sony; Accudrop beads, BD), typical of traditional FACS workflows for cellular analysis. Bead-calibrated drop delay values and starting droplet spacing, droplet profile, and drop-drive frequency were recorded as set points before manual droplet delay calibration. Manual adjustment of the droplet delay had minimal effects on droplet recovery efficiencies for the SH800; intital droplet delay values were used for all SH800 sorts. For the Aria II, we observed a significant effect on sorting efficiency upon adjustment of the droplet delay (see **Fig. S7**, and Extended Notes). A manual droplet delay adjustment using control DE populations prior to each run was performed on the Aria II. Confirmatory droplet delay calibrations can be confirmed on either instrument, as desired.

Protocol for Manual Droplet Delay Adjustment:
Run time: 5-7 min

1. Generate droplets for manual droplet delay adjustment by either (1) setting aside a small split-fraction of your droplet sample (dedicated for calibration-only) or (2) generate a small (~20 μL pellet, 2-4 min generation time) control droplet population using the same flow rates (recommended for rare or precious samples). Calibration droplets must have a similar total volume and oil shell size, as these parameters influence the resultant DE-optimized droplet delay.

2. Calibrate the cytometer using standard flow cytometry beads and note the drop delay set point.

3. Load the chosen calibration droplet population and gate according to FSC vs. SSC morphology.

4. Load an optical 96-well plate into the plate loader. Each well in 1 row should contain 100 μL of outer aqueous sheath buffer to stabilize the sorted droplets.

5. Using the instrument software, manually adjust the drop delay units on the droplet profile from the set point by -1.5 to +1.5 in 0.25 – 0.5 unit increments, as in **Fig. S7**.

> 5.a. For each increment, sort 50 droplets with single cell purity into a well of the 96-well plate. Note the well location and droplet delay per each sort.
>
> 5.b. Wait 10 s during active event collection at the new droplet before proceeding to the next sort. This stabilizes target selection to ensure droplets of the right drop delay enter the well.
>
> 5.c. If FACS droplet profiles, droplet-drive settings, or spacing become unstable, wait for stabilization or adjust the parameters until stabilization is regained. Droplet delay profiles must be collected under stable FACS droplet breakoff.

6. When the droplet delay calibration sort has been completed, manually count each well using a benchtop stereoscope (Amscope). This step should take 2-3 min total. Automated imaging is possible (e.g., using an EVOS plate microscope, Life Technologies) but is not necessary.

7. Select the adjusted droplet delay profile with the maximal number of droplets collected in the sweep. Successful calibrations should achieve 50 – 90% sort recovery efficiency; set point recovery efficiencies are predict later sort statistics for the population. Proceed with all further sorting and analysis using the new droplet delay.

We have found manually-calibrated drop delays (as expressed relative to the Accudrop-calibration value, ***e.g.*** +0.5 d.d. units) are extensible to DEs of the same droplet size and chemistry.

3. Droplet Size Analysis

Droplets were imaged for size characterization on a Nikon Ti Eclipse microscope at 10X under brightfield and a fluorescence channel according to a reference dye in each droplet. In this work, FITC was used as the reference dye. Multiple images were analysed per droplet population (typically, 5 – 20 images per condition, 50 – 500 droplets analysed total per condition). An automated pipeline was developed in MATLAB to

extract radial and volumetric information about the droplets. First, a central ROI of 500 x 500 pixels was extracted from each droplet image. In the FITC channel image, center coordinates and radii of all inner cores were obtained using the circular Hough transform method (imfindcircles). In the brightfield channel image, each droplet was isolated in a square ROI centered at the x- and y-coordinates of the extracted droplet centroid, as determined from the fluorescence image, with each side twice the length of the inner core's radius. The droplet ROI was contrast-enhanced and coverted to grayscale through contrast-limited adaptive histogram equalization (adapthisteq). An image profile of pixel intensities was taken along the horizontal and vertical center lines of the ROI (improfile). Given that the outer boundary of a droplet has low pixel intensity relative to its surroundings, intensity and positional information of local minima (identified using peakdet) in the image profiles were extracted. By direct comparison of the coordinates of the first and last minima in the horizontal and vertical profiles, the two positions closest to the droplet's center were selected to demarcate the outer shell's boundaries. If the two minima originated from different image profiles (i.e. one from the horizontal profile, and the other from the vertical profile), positions were standardized by converting the last minimum to the minimum closest to its original position on the other image profile. The droplet diameter was reported as the difference between the two extracted minima. To correct overlapping droplet boundaries, the difference between the sum of the overlapping droplets' radii and the Euclidean distance between their centers was subtracted from each droplet's radius. Droplets whose outer radii were found to be smaller than their inner radii were removed from consideration. Through visual inspection, droplets were excluded from analysis during outer shell boundary detection if a local minima could not be identified for a given droplet due to close droplet packing (typical rejection rate: 10%, random sampling).

Droplet sizes were manually quantified in samples lacking a reference dye (e.g., PBS Blank droplets, **Fig. 2**). Brightfield images were opened in ImageJ, and circular regions of interest were manually drawn around each inner core and outer shell visible in an image. For each population, 50 identified droplets were randomly sampled and reported for size characterization; ROI coordinates and masks were saved and recorded for each population.

4. Droplet Taqman PCR and Thermocycling

To that sdDE-FACS is compatible with thermocycling reactions, we performed in-droplet genomic Taqman PCR in double emulsions as described in Sukovich et al., 2017[1] and subsequently sorted Taqman-positive droplets using the sdDE-FACS technique. Lambda DNA (NEB) and Phi X174 DNA (NEB) were diluted in qPCR-grade water (Invitrogen) prior to use. A PCR reaction was assembled as follows: 25 μL Platinum Multiplex PCR Master Mix (Thermo Fischer), 2.5 μL Taqman probe (5 μM), 0.5 μL forward primer (100 μM), 0.5 μL reverse primer (100 μM), 2 μL diluted DNA, 5 μL UltraPure BSA (5% stock, Ambion), and qPCR-grade water (Invitrogen) to 50 μL. A separate mix was prepared for each DNA sample. The PCR mix was loaded into a single-inlet device to generate ~30 μm double emulsions; flow rates were 275:75:2500 (O:I:S) μL/hr. After collection, droplets were supplemented with 2X Taq Polymerase reaction buffer (Thermo Fisher) and 1.5 mM $MgCl_2^{2+}$ in 1:1 dilution with the outer aqueous phase and subjected to Taqman PCR cycling using a Life Technologies thermocycler according to the following program: (86C for 2 min; 40 x 86C for 30s, 60C for 90s, 72C for 20s; 72C for 5 min). Post-cycling droplets were imaged using a Nikon TiEclipse under brightfield and FAM fluorescence. Droplets containing either lambda DNA (NEB) and Phi X174 DNA (NEB), and associated probes and primers, were mixed 1:100 in the droplet sample and analysed via FACS, with target enrichment for the positive population. Droplets were subsequently imaged post-recovery for direct comparison on the performance of the sdDE-FACS workflow to Sukovich et al., 2017[1].

Extended Discussion Notes

1. Double Emulsion Generation

We generated double emulsions were generated using 3 syringe pumps (Pico-Pump Elite, Harvard Apparatus) for the inner aqueous, oil, and outer carrier fluids as shown in **Fig. S1**. Additional syringe pumps and sample loaders (e.g., sample loops, paired syringe pumps, stopcock assemblies) can be added, as desired, for additional inner core reagents (e.g., reaction mixes, lysis buffers, cell dyes, etc.) or reagent exchange dependent on the design of the microfluidic device. Syringes can be selected for either normal-volume (1 – 5 mL; PlastiPak plastic syringes, BD) or low-volume (10 – 500 uL; Hamiliton glass syringes, Sigma) applications per reagent. We recommend the use of polyethylene tubing (PE/2, Scientific Commodities) because of its low-bind properties and biological compatibility, but Tygon, FEP, or alternative polymer tubing are also attractive options. A full description of setup components is available in **Table S1**; costs are typically between $7,000 - $10,000 for setup construction with <$10 consumables per device array (10 – 15 runs per array). Droplet generation rates are typically 1-10 kHz, with 0.6 - 6M droplets collected per each 10 min run time for 30 μm droplets. Higher or lower collection rates can be achieved with smaller or larger size droplets, respectively.

2. Double Emulsion Device

The device design used in this work is similar to a previously reported dual flow-focuser design[2,3]. In this design, single emulsions containing an inner aqueous core are first generated in an oil sheath (flow focuser #1) and subsequently enveloped in an oil shell by the second aqueous sheath (flow focuser #2), separated by a flow resistor channel of high fluidic resistance to stabilize the two flow regimes. This device allows highly uniform, reproducible droplet generation using an easy 'one-step' approach (e.g., all inlets are plugged into the same singular device and run simultaneously to produce resultant double emulsions). We have fabricated multiple variants of the 'one-step' dual-focuser device presented in this work containing a varying number of inlets for different reaction schemes, or different channel heights (***e.g.,*** a 25 μm inner flow focuser, 50 outer flow focuser device for 40 μm droplet generation presented in **Fig. S4, S5**). The device is robust to translation across different droplet size regimes, and easy to adopt in different workflows. Alternative commercial devices or different device geometries are also compatible with sdDE-FACS.

3. Double Emulsion Device Wettability

To generate differential wettability between the first and second flow focuser of the 'one step' dual-flow focuser droplet generator device, we employ selective air or oxygen plasma treatment (4.5 min, 150W O_2 plasma) on the inlets associated with the outer aqueous flow focuser (outer aqueous sheath inlet and outlet) using the tape method described previously[4]. Alternative surface treatments can be employed, if desired. Resultant double emulsions need only be relatively uniform (CV: <20%) and lacking significant free oil (by employing sdDE-FACS surfactant suggestions and adjusting flow rates).

4. Double Emulsion Surfactants

A table of surfactants used for sdDE-FACS is presented in **Table 1**. Any base buffer (***e.g.*** PBS, water, media, etc.) can be used for these surfactant formulations with no adverse effects as long as serum and other surfactants are removed or minimized. Optionally, BSA (0.5-2%) can be substituted for inner core Tween-20 (0.1-1%) with no adverse effects; this substitution may be desirable for cellular studies where viability is important.

5. FACS Analysis of Double Emulsions Extended Note

During FACS, DE droplets are diluted in a diluent suspension buffer and loaded into the instrument, where they meet a fast-moving sheath buffer (with typical flow pressures of 1-10 psi). This sheath flow hydrodynamically focuses DE droplets and carries them into a flow cell where they are excited by a series of lasers for quantitative phenotyping. After laser interrogation, the sheath flow is acoustically aerosolized to create water-in-air droplets ("FACS droplets", 6.9 nL for a 130 μm nozzle) that encapsulate DE droplets for sorting (now a triple-droplet architecture). Immediately prior to aerosolization, the sheath fluid is charged (by the charge wire, CW, **Fig. 2B**) if a droplet-of-interest meeting a phenotypic gate criteria is detected. This charge is imparted on the aerosolized DE-containing "FACS droplet" for electrostatic deflection into wells. Only targeted droplets receive a charge; DEs not meeting the selected gate are directed to waste. The charge timing is decided by an important sorting parameter, called droplet delay (DD, **Fig. 2B**), , which sets the delay time between when a DE droplet passes through the laser excitation and when charge is applied to target droplets after they leave the nozzle and reach the stable breakoff. Drop delay depends on particle size and hydrodynamics in the sort stream. Droplet delay must be determined empirically for reliable sorting (**Fig. S7**). Robust recovery of DE droplets requires that all droplets remain intact throughout this process to prevent cross-contamination (***e.g.,*** through breakage in the flow stream or FACS droplet spray).

6. Droplet Dilution Extended Note

Population 'purity' during sorting (***i.e.*** the percentage of events in the DE FSC ***vs.*** SSC gate) depends strongly on the absolute number droplets loaded into FACS diluent buffer (total volume: 600 uL), as highlighted in SH800 (Sony) data with highly permissive threshold and gain settings (**Fig. S2)**. Events in the lower left corner of this FSC ***vs.*** SSC plot indicate dust and small surfactant micelles that comprise ~38% of the parental population (with DEs comprising the remaining 61.6%, 30,000 total events in parental population on both Aria II and SH800). These results are typical for runs in which 50 – 100 μL are loaded from the droplet pellet (~0.2 – 5M droplets, dependent on size). Loading smaller numbers of DEs reduces overall throughput and may increase the need to manually resuspend DEs during a FACS run. Conversely, loading larger numbers of DEs can increase breakage through elastic collisions between DEs (particularly on the SH800) and therefore requires careful monitoring of droplet singlet rates over time. Events/second rates > 2,000 generally signify breakage and that the sort pressure should be decreased or the run should be aborted. In any case, subsequent gating allows stringent isolation of DEs from contaminants, rendering sdDE-FACS compatible with both scarce biological samples and abundant samples containing rare variants of interest.

7. Droplet Lag Time

On the SH800, after the start of a run there is typically a 'lag' time prior to the appearance of double emulsion droplets as shown in **Fig. S3**. On average, DEs are observed within the relevant FSC vs. SSC gate by 20s for the Aria II but can take up 1 – 4 min for the SH800, with a strong dependence on initial loading droplet density, droplet size and sort pressure. In order to boost initial events in the SH800, we begin all flow cytometry double emulsion runs at 9 psi until events begin to appear in the DE gate; after their appearance, droplet events tend to rise exponentially (as shown in **Fig. S3**). Subsequently, we modulate the sort pressure between 4 – 9 psi, corresponding to droplet density, to cap the event rate below 200 events/s. The SH800 uses a microfluidic chip with a laminar flow regime rather than the quartz cuvette with a hydrodynamic flow focusing regime employed by the Aria II. Observed droplet event delay and subsequent rapid boosting may be due to droplet packaging within the microfluidic sort chip or sample line. Double

emulsions are highly deformable; similar effects have been observed and utilized for hydrogel packing regimes in microfluidics to achieve highly-regular flow metering after packing.

8. BD Aria II: Flow Cell Effects

The Aria II can be operated with a rectangular or square flow cell. Square flow cells observe "plug flow" behaviour and have excellent performance for large cell samples. sdDE-FACS performs well with either flow cell; a mixed population enrichment experiment is highlighted in **Fig. S8** using the square flow cell. All other experiments reported in this work were conducted with a rectangular flow cell.

9. SH800: Size Differentiation Effects

DEs can be easily discriminated by overall droplet size using the sdDE-FACS technique as shown in **Figs. S4, S5,** and **S6**. Size discrimination between 30 μm and 40 μm droplet populations is most apparent on FSC-A ***vs.*** SSC-A plots. Within populations, large droplet sizes (40 μm) can be more readily differentiated by inner volume and oil shell thickness (**Fig. S6**), especially using the SSC-A parameter which is able to parse 3 distinct scatter distributions corresponding to the 3 oil shell sizes shown in **Fig. S5**. This discrimination is pulse-width dominant (FSC-W and SSC-W effects are most significant in FSC-A and SSC-A discrimination).

References

1. Sukovich, D. J., Lance, S. T. & Abate, A. R. Sequence specific sorting of DNA molecules with FACS using 3dPCR. ***Scientific Reports*** **7**, (2017).
2. Lim, S. W. & Abate, A. R. Ultrahigh-throughput sorting of microfluidic drops with flow cytometry. ***Lab on a Chip*** **13**, 4563 (2013).
3. Abate, A. R., Thiele, J. & Weitz, D. A. One-step formation of multiple emulsions in microfluidics. ***Lab Chip*** **11**, 253–258 (2011).
4. Abate, A. R., Thiele, J., Weinhart, M. & Weitz, D. A. Patterning microfluidic device wettability using flow confinement. ***Lab on a Chip*** **10**, 1774 (2010).
5. Hai, M., Bernath, K., Tawfik, D. & Magdassi, S. Flow cytometry: a new method to investigate the properties of water-in-oil-in-water emulsions. ***Langmuir*** **20**, 2081–2085 (2004).
6. Aharoni, A., Amitai, G., Bernath, K., Magdassi, S. & Tawfik, D. S. High-Throughput Screening of Enzyme Libraries: Thiolactonases Evolved by Fluorescence-Activated Sorting of Single Cells in Emulsion Compartments. ***Chemistry & Biology*** **12**, 1281–1289 (2005).
7. Mastrobattista, E. ***et al.*** High-Throughput Screening of Enzyme Libraries: In Vitro Evolution of a β-Galactosidase by Fluorescence-Activated Sorting of Double Emulsions. ***Chemistry & Biology*** **12**, 1291–1300 (2005).
8. Yan, J. ***et al.*** Monodisperse Water-in-Oil-in-Water (W/O/W) Double Emulsion Droplets as Uniform Compartments for High-Throughput Analysis via Flow Cytometry. ***Micromachines*** **4**, 402–413 (2013).
9. Zhang, Y. ***et al.*** A programmable microenvironment for cellular studies via microfluidics-generated double emulsions. ***Biomaterials*** **34**, 4564–4572 (2013).

10. Zinchenko, A. ***et al.*** One in a Million: Flow Cytometric Sorting of Single Cell-Lysate Assays in Monodisperse Picolitre Double Emulsion Droplets for Directed Evolution. ***Analytical Chemistry*** **86**, 2526–2533 (2014).

11. Ma, F., Xie, Y., Huang, C., Feng, Y. & Yang, G. An Improved Single Cell Ultrahigh Throughput Screening Method Based on In Vitro Compartmentalization. ***PLoS ONE*** **9**, e89785 (2014).

12. Ma, F. ***et al.*** Substrate Engineering Enabling Fluorescence Droplet Entrapment for IVC-FACS-Based Ultrahigh-Throughput Screening. ***Analytical Chemistry*** **88**, 8587–8595 (2016).

13. Larsen, A. C. ***et al.*** A general strategy for expanding polymerase function by droplet microfluidics. ***Nature Communications*** **7**, 11235 (2016).

14. Lance, S. T., Sukovich, D. J., Stedman, K. M. & Abate, A. R. Peering below the diffraction limit: robust and specific sorting of viruses with flow cytometry. ***Virology Journal*** **13**, (2016).

15. Chan, H. F., Ma, S., Tian, J. & Leong, K. W. High-throughput screening of microchip-synthesized genes in programmable double-emulsion droplets. ***Nanoscale*** **9**, 3485–3495 (2017).

16. Sukovich, D. J., Kim, S. C., Ahmed, N. & Abate, A. R. Bulk double emulsification for flow cytometric analysis of microfluidic droplets. ***The Analyst*** **142**, 4618–4622 (2017).

17. Terekhov, S. S. ***et al.*** Microfluidic droplet platform for ultrahigh-throughput single-cell screening of biodiversity. ***Proceedings of the National Academy of Sciences*** **114**, 2550–2555 (2017).

Supplemental Figures:

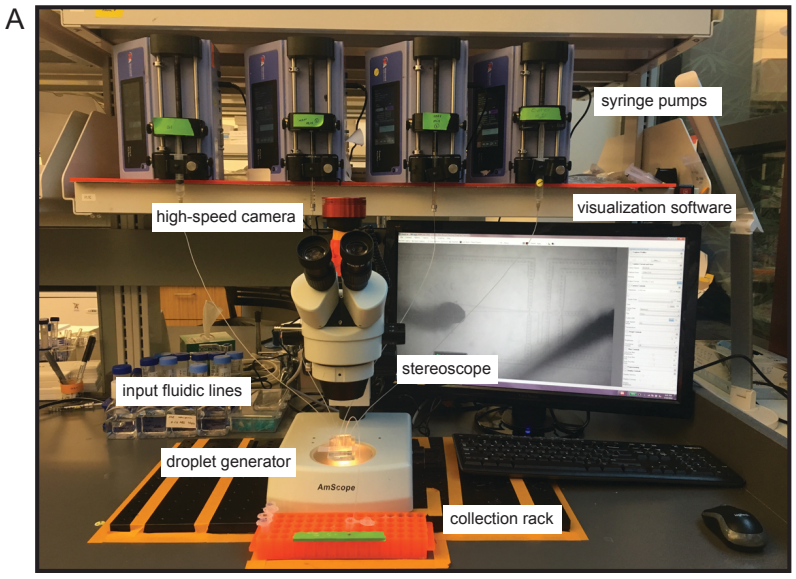

Figure S1: Double emulsion generation setup for sdDE-FACS workflow. **(A)** Double emulsion generation setup (~$10,000) comprised of syringe pumps, a microfluidic droplet generator device, a stereoscope and high-speed camera for droplet visualization, and a collection rack for holding generated droplets. Syringes loaded with reagents are connected to device inlets via polyethylene (PE) tubing, and device outlet is connected to a collection tube via a short segment of PE tubing to collect droplets.

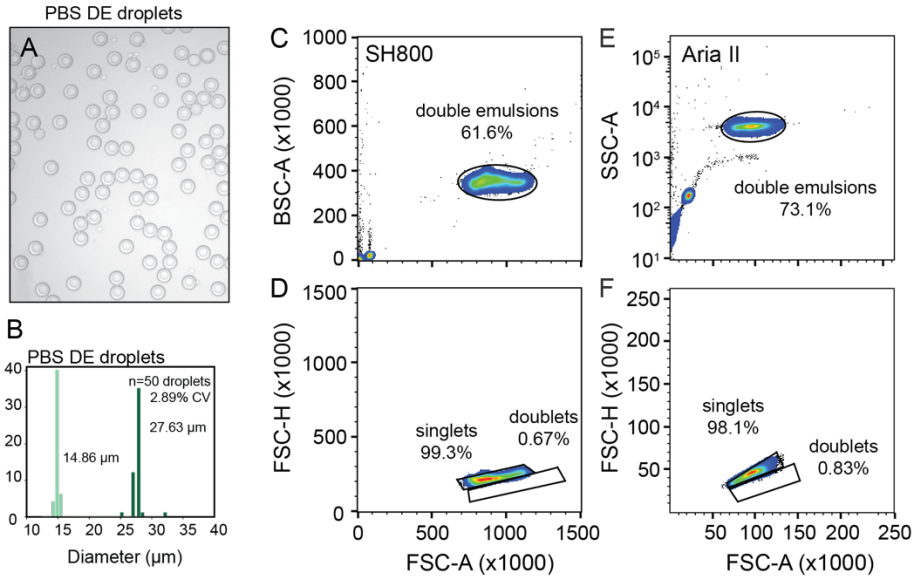

Figure S2: Representative sdDE-FACS analysis results for 30 µm droplets. **(A)** Brightfield image of DE droplets loaded with PBS buffer. **(B)** Population size histogram (light green = inner diameter, dark green = outer diameter, mean diameters indicated). **(C, D)** FACS morphology and singlet discrimination gates for the SH800. **(E, F)** FACS morphology and singlet discrimination gates for the Aria II. 30,000 events are shown for each parental gate; events were randomly downsampled.

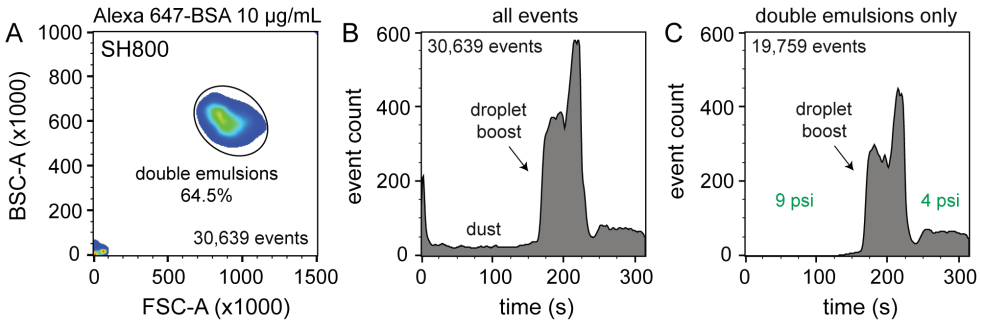

Figure S3: Typical delay times before the appearance of DE droplets on the SH800 (Sony). **(A)** Representative DE population as shown on the FSC ***vs.*** BSC morphology gate (SH800). **(B)** Total events per time shown for the full parental population of (A). **(C)** Events appearing in the double emulsion gate shown in (A). Note that dust events (shown in the lower left corner of (A)) dominate for the first ~160s of the FACs run. After ~160s, DE droplets begin to appear and event rates rise rapidly. Pressure was run at 9 psi (instrument limit = 10 psi per 130 µm nozzle) until the droplet event boost was observed. When a significant droplet population was visualized for gating, sheath pressure was decreased to 4 psi to attain a sort rate below 200 events/s for optimal droplet integrity post-sort.

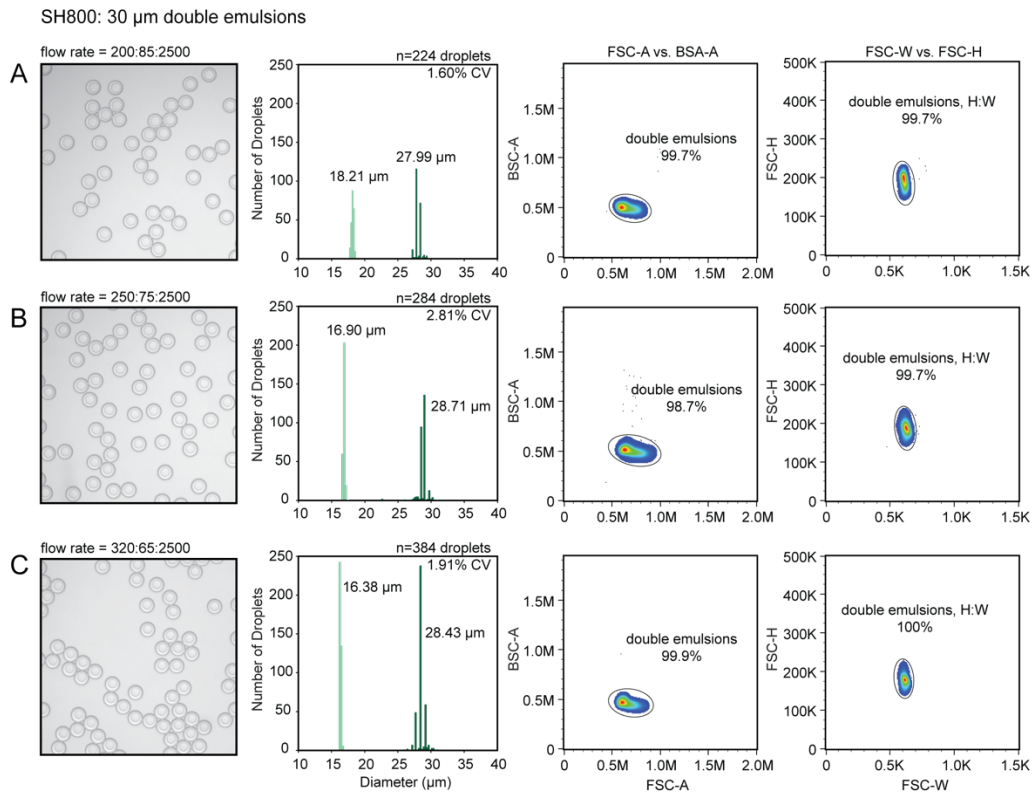

Figure S4: Size discrimination using sdDE-FACS on the SH800 (Sony) sorter, **Part I**. Comparative FACS analysis of 30 µm DE droplets with 3 different oil shell thickness resulting from different droplet flow rates (oil: inner core: outer aqueous sheath) of **(A)** 200:85:2500, **(B)** 250:75:2500, and **(C)** 320:65:2500. Representative brightfield images (left) and size histograms (light green = inner diameter, dark green = outer diameter, middle left) show population monodisperity and size differences between conditions. Ratio of inner core volume to total volume of the droplet are as follows for each condition: **(A)** 0.45, **(B)** 0.30, and **(C)** 0.24. FSC-A vs. BSC-A (middle right) and FSC-H vs. FSC-W (right) FACS plots for each condition (downsampled randomly to 1500 events per population) demonstrate that oil shell size only has minor effects on differential FSC or BSC in the 30 µm droplet populations.

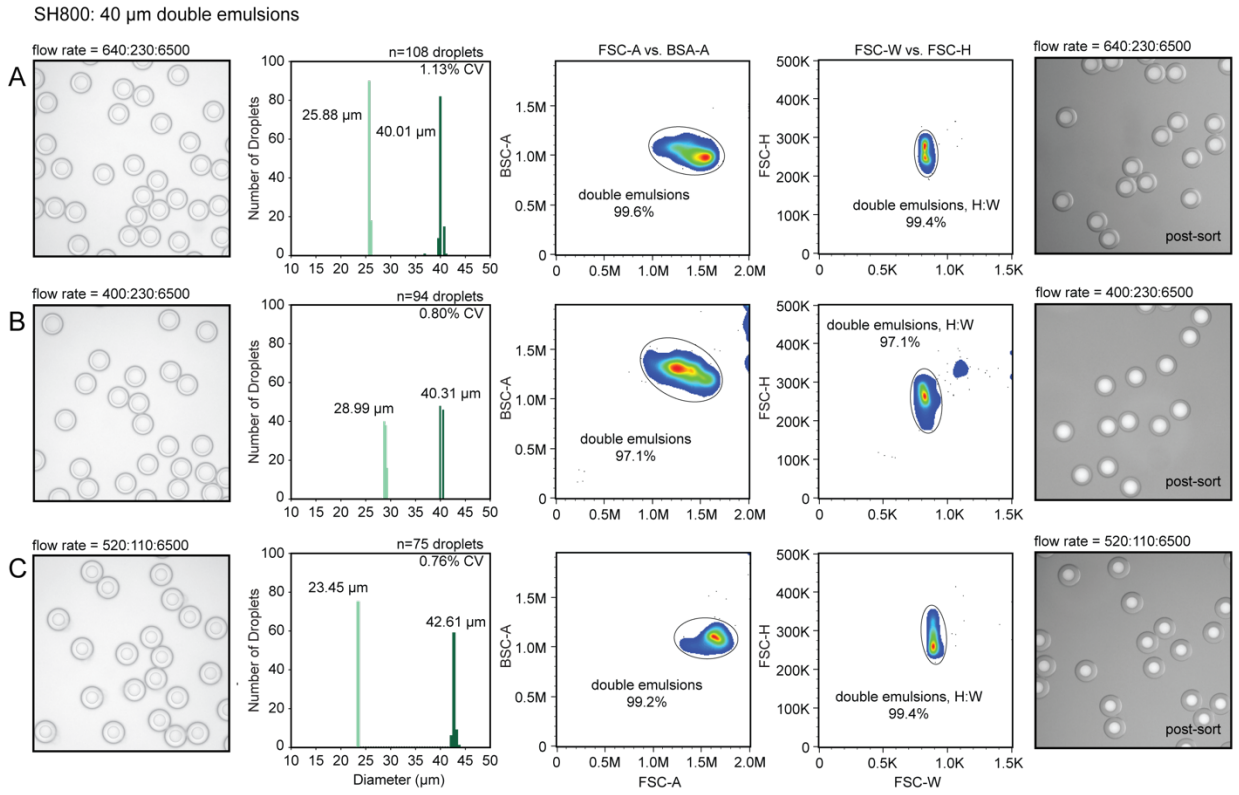

Figure S5: Size discrimination using sdDE-FACS on the SH800 (Sony) sorter, **Part II**. Comparative FACS analysis of 40 µm DE droplets with 3 different oil shell thickness resulting from different droplet flow rates (oil: inner core: outer aqueous sheath) of **(A)** 640:230:6500, **(B)** 400:230:6500, and **(C)** 520:110:6500.. Representative brightfield images (left) and size histograms (light green = inner diameter, dark green = outer diameter, middle left) show population monodisperity and size differences between conditions. Ratio of inner core volume to total volume of the droplet are as follows for each condition: **(A)** 0.37, **(B)** 0.59, and **(C)** 0.20. FSC-A vs. BSC-A (middle right) and FSC-H vs. FSC-W (right) FACS plots for each condition (downsampled randomly to 1500 events per population) demonstrate that oil shell size has large effects on differential FSC or BSC in the 40 µm droplet populations.

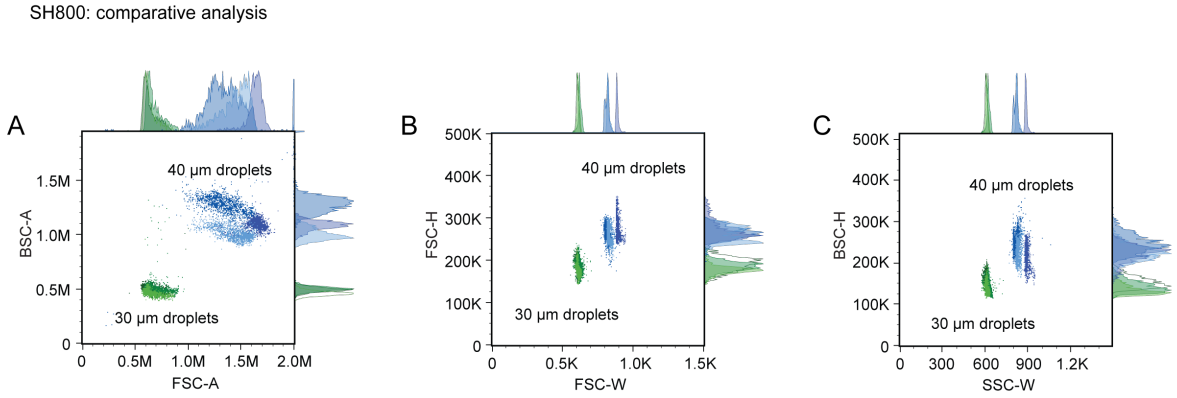

Sample Name	Count	Median : FSC-A	Robust SD : FSC-A	Median : SSC-A	Robust SD : SSC-A
640_230_6500	1500	1.46E6	133789	9.92E5	59708
520_110_6500	1500	1.64E6	54443	1.08E6	42818
400_230_6500	1500	1.33E6	161865	1.28E6	73981
320_65_2500	1500	6.25E5	60303	4.59E5	22361
250_75_2500	1500	6.63E5	76904	5.00E5	23312
200_85_2500	1500	6.23E5	68115	4.92E5	21885

Figure S6: Comparative analysis of sdDE-FACS data 30 µm (**Fig. S4**) vs. 40 µm (**Fig. S5**) droplet populations. **(A)** FSC-A vs. BSC-A, **(B)** FSC-H vs. FSC-W, and **(C)** BSC-H vs. BSC-W distributions by condition reveal clear separation between 30 and 40 µm droplets and high inter-size discrimination on BSC-A for large droplets (40 µm population), with dominant effects from pulse-width discrimination. See further discussion in ***Extended Notes***.

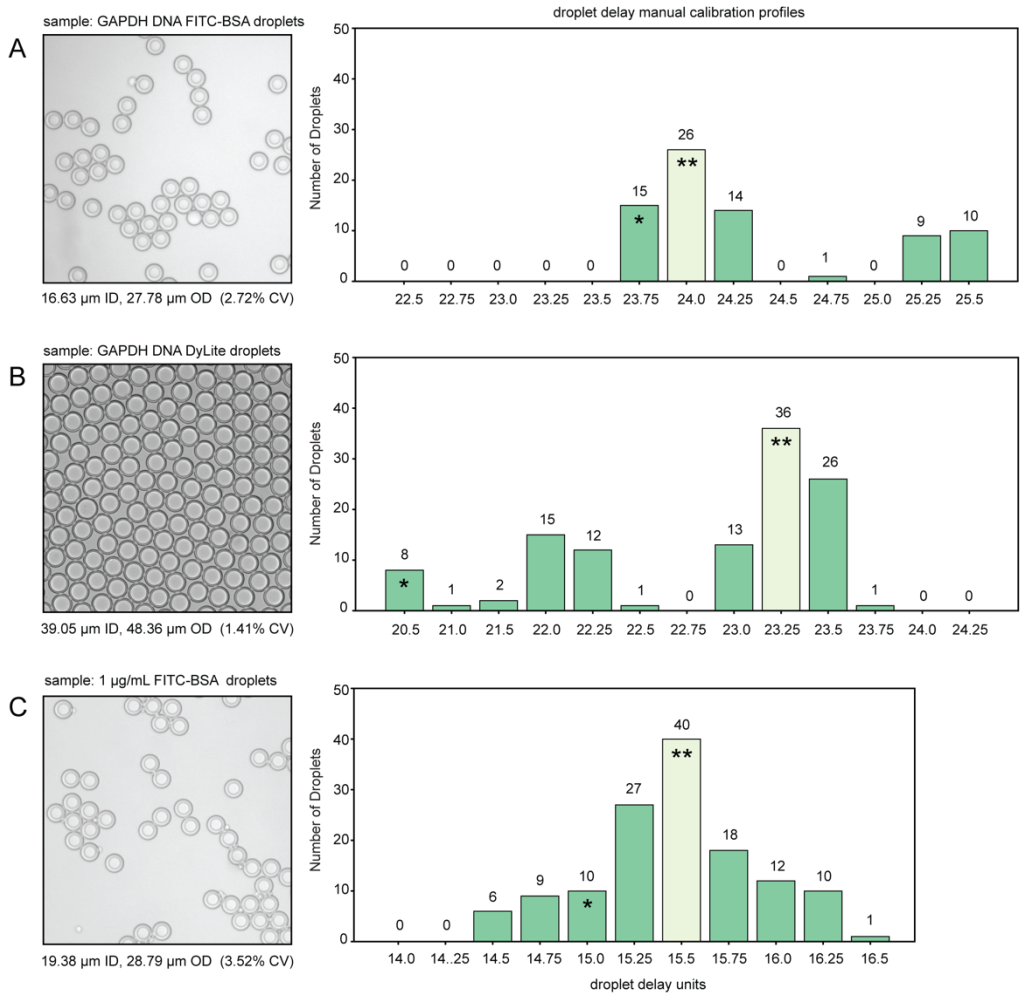

Figure S7: Representative droplet delay profiles from empirical droplet delay determination for 30-50 µm DEs on the Aria II. Manual delay profiles are shown for: **(A)** GAPDH-DNA loaded double emulsions with FITC-BSA dye (27.8 µm), **(B)** small-shell GAPDH-DNA loaded double emulsions with DyLite Antibody (Cy5) dye (48.4 µm), and **(C)** FITC-BSA reference droplets (28.9 µm). Each histogram was calculated for a manual droplet delay sweep outlined in ***Extended Methods.*** Each bar of the histogram corresponds to number of observed droplets in a well designated to receive 50 DE droplets at the indicated droplet delay. Accudrop-calibrated droplet delays and empirically determined drop delays are denoted by (*) and (**), respectively.

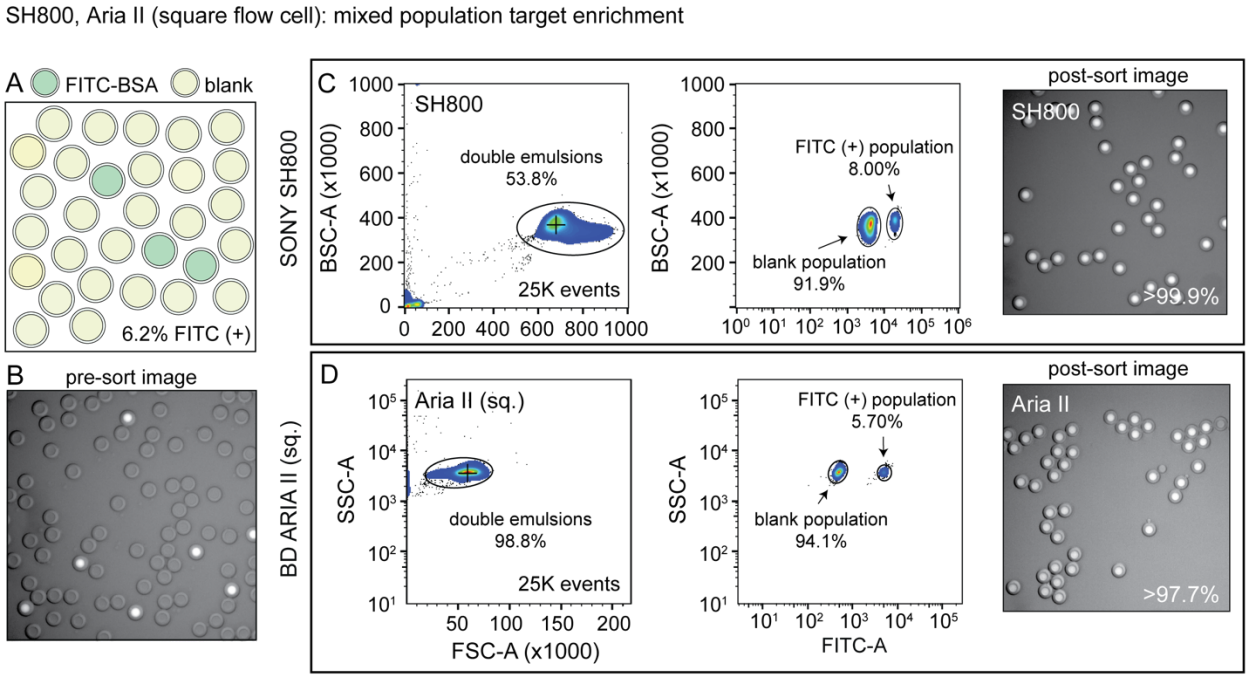

Figure S8: Replicate target enrichment experiment from a mixed parental population similar to **Fig. 4** conducted a square flow cell on the Aria II with manually-adjusted droplet delay. FITC-positive droplets were enriched with high specificity from a mixed population containing of 6.2% FITC-BSA positive DEs and blank DEs **(A, B).** High target specificity and sensitivity were observed on an Aria II instrument containing a square flow cell, comparable to rectangular flow cell results (**Fig. 4**). See further discussion in ***Extended Notes***.

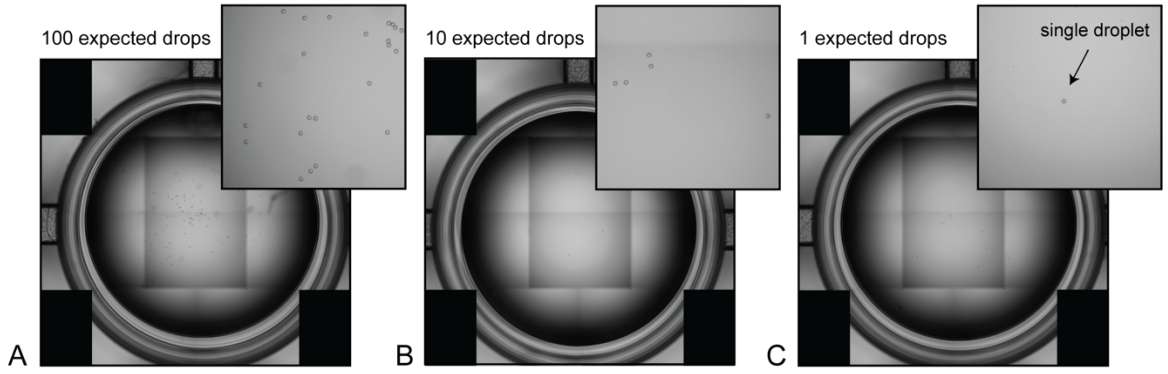

Figure S9: Example EVOS (Life Technologies) microscopy images used to calculate DE-FACS recovery rates using the Aria II sorter for **(A)** 100- , **(B)** 10-, and **(C)** 1- droplet set points. Each panel displays a full-well image (left) and magnified 600 x 600 pixel region of interest (top right).

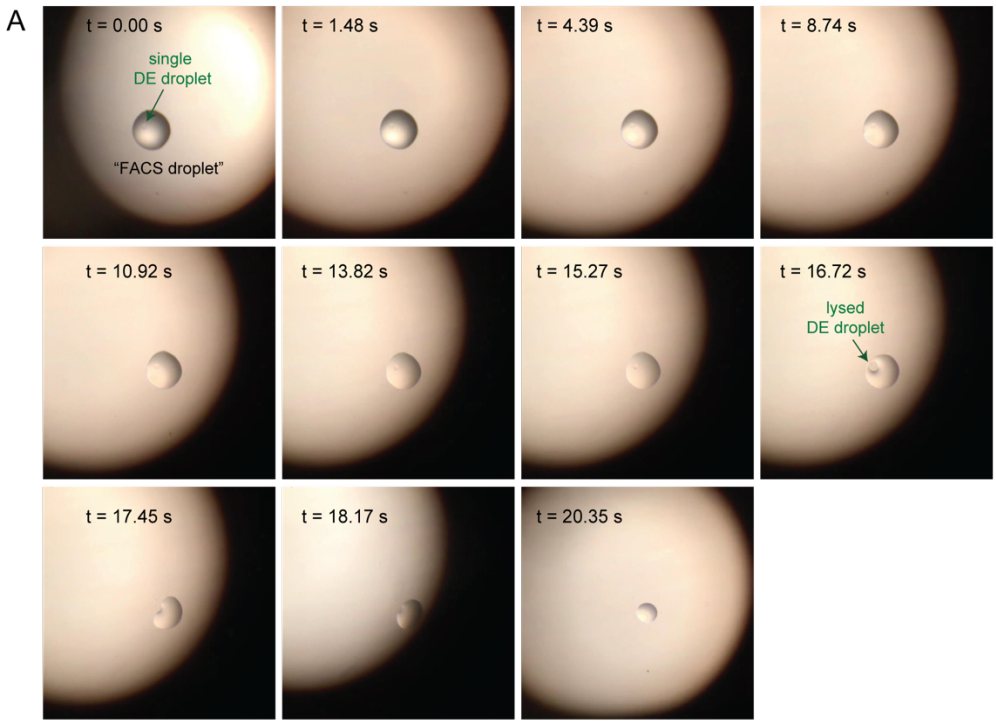

Figure S10: Image sequence of on-plate droplet lysis within a single 'FACS droplet' deposited in a dry well of a 96-well plate. Dry droplet lysis was employed for nucleic acid recovery as presented in **Figs. 6, S11.**

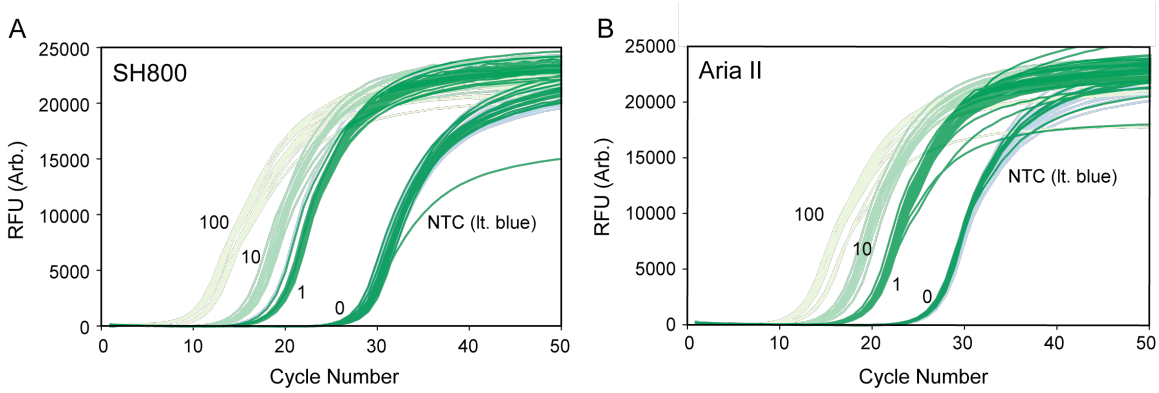

Figure S11: Raw qPCR traces using sdDE-FACS with two flow cytometer instruments: **(A)** SH800 (Sony), and **(B)** Aria II. qPCR traces are for 96-well full-plate nucleic acid recovery (standards omitted).

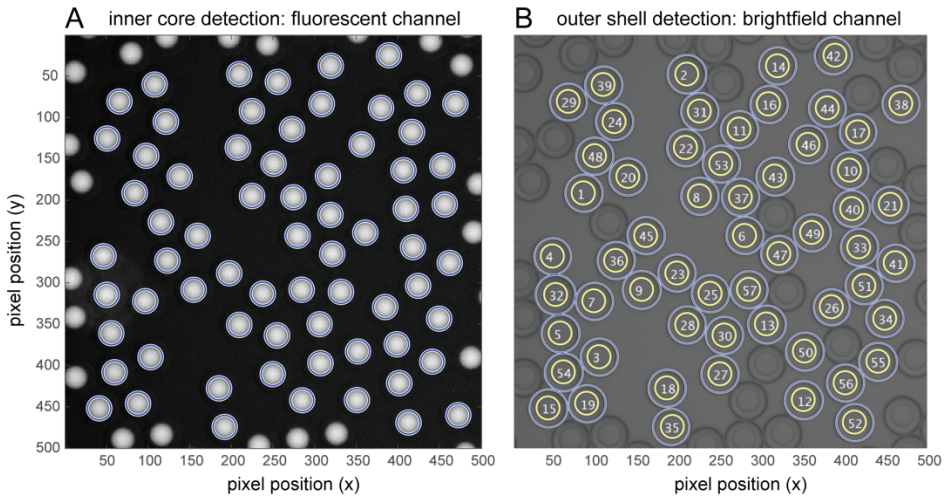

Figure S12: Automated DE droplet detection and inner and outer droplet size measurement. **(A)** A modified Hough transform algorithm allows automated droplet identification and measurement of inner core diameters from a reference dye fluorescent channel image, as shown here for DE droplets containing FITC-BSA. **(B)** Outer shell boundaries are identified by performing a line scan centered on the fluorescence centroid position and searching for intensity minima in the greyscale image. Droplets are indexed by condition, image number, and droplet count, as shown; overlapping or adjacent droplets are omitted from subsequent size analysis.

Supplemental Tables:

Table S-T1:

Setup Component	Supplier	Cost
Syringe pumps	Pico Pump Elite, Harvard Apparatus	$3,083.00 x 3
High-frame rate camera	ASI 174MM, ZWO ASI	$599.00
Visualization software	SharpCap, ZWO ASI	$0.00
Computer	Generic laptop, Lenovo	$650.00
PDMS Device	RTV 615, Momentive (***per chip***)	$3.00
Microfluidic tubing	PE/2, Sci. Commodities (***per spool)***	$83.00
Syringes, disposable	1 mL, 5 mL Plasti-pak, BD (***per run***)	$6.00
	Total	$10,590.00

Table S-T1: Components and associated suppliers for building and operating the droplet generation setup shown in **Figure S1**. Note: the syringe pumps listed (Pico Pump Elite, Harvard Apparatus) are utilized specifically for high-precision, low-volume applications (10 – 500 μL/hr); alternative suppliers can be used (New Era Pumps, $1,500/pump) to reduce costs if desired. Costs current as of October 2019.

Table S-T3:

Assay	Sorter	Sample	Set Point (Expected No. of Droplets)			
			100 droplets	10 droplets	1 droplet	0 droplet
Optical	Aria II*	GAPDH DyLite	71.2 (5.6) N=11 wells	6.1 (2.2) N=36 wells	0.50 (0.51) N=24 wells	0 (0) N=25 wells
Optical	SH800	GAPDH DyLite	69.9 (4.5) N=12 wells	7.1 (1.5) N=36 wells	0.71 (0.50) N=24 wells	0 (0) N=24 wells
Optical	Aria II*	Plate 1 FITC-BSA	81.9 (4.0) N=12 wells	6.9 (3.5) N=12 wells	0.83 (0.38) N=48 wells	1 (0) N=24 wells
Optical	Aria II*	Plate 2 FITC-BSA	83.6 (2.7) N=12 wells	8.4 (1.2) N=12 wells	0.83 (0.38) N=48 wells	0 (0) N=24 wells
Optical	SH800	Plate 1 FITC-BSA	55.5 (3.4) N=12 wells	5.3 (1.8) N=12 wells	0.75 (0.48) N=48 wells	0 (0) N=24 wells
Optical	Aria II*	Plate 1 GAPDH DyLite	64.4 (7.9) N=12 wells	5.9 (1.7) N=12 wells	0.77 (0.47) N=48 wells	0 (0) N=24 wells
Optical	Aria II*	Plate 2 GAPDH DyLite	64.8 (7.2) N=12 wells	6.3 (1.7) N=12 wells	0.56 (0.61) N=48 wells	0 (0) N=24 wells
Optical	SH800	Plate 1 GAPDH DyLite	46.2 (8.2) N=12 wells	4.9 (1.4) N=12 wells	0.56 (0.50) N=48 wells	4 (0) N=24 wells
Optical	Aria II*	***Singles-Only*** GAPDH DyLite	0 (0) N=0 wells	0 (0) N=0 wells	0.80 (0.40) N= 96 wells	0 (0) N=0 wells
qPCR	SH800	Plate 1 DNA-FITC-BSA	N/A (--) N=0 wells	N/A (--) N=0 wells	0.53 (--) N=19/36 wells	N/A (--) N=0 wells
qPCR	SH800	Plate 2 DNA-FITC-BSA	N/A (--) N=0 wells	N/A (--) N=0 wells	0.69 (--) N=25/36 wells	N/A (--) N=0 wells
qPCR	Aria II*	Plate 1 DNA-FITC-BSA	N/A (--) N=0 wells	N/A (--) N=0 wells	0.61 (--) N=22/36 wells	N/A (--) N=0 wells
qPCR	Aria II*	Plate 1 DNA-FITC-BSA	N/A (--) N=0 wells	N/A (--) N=0 wells	0.66 (--) N=23/35 wells	N/A (--) N=0 wells

Table S-T3: Extended plate statistics. Manual droplet delay calibration is indicated by (*). qPCR readouts contain 100, 10, 1 and NTC wells as indicated in **Figs. 6, S11**; however, binary sort statistics corresponding to droplet presence of absence (as determined by C_q cluster and expected [DNA]) are only accessible for single droplet deposition wells (n=36 wells/plate) and are reported here as fraction of total occupied single-droplet set point wells.

Table S-T4:

Oligonucleotide	Sequence
GAPDH 175-bp DNA fragment	ACCACAGTCCATGCCATCACTGCCACCCAGAAGACTGTGGAT GGCCTGTGGCGTGATGGCCGCGGGGCTCTATCAAGAAGGTG GTGGCTACACTGAGCACTGCCCTCAACGACCACTTTGTCAAG CTCATTTCCTGGTATGACAACGAATTTGGCTACAGCAACAGG GTGGTGGA
GAPDH primer, forward	ACCACAGTCCATGCCATCAC
GAPDH primer, reverse	TCCACCACCCTGTTGCTGTA

Table S-T4: Oligonucleotides used for DE nucleic acid recovery qPCR experiments described in **Fig. 6** and **Fig. S11**.

Table S-T5:

Reaction Component	Volume ***per well***	Final Concentration
2X iTaq SYBR qPCR Mix (Biorad)	5 uL, 1X	1X
10 μMGAPDH primer, forward	0.25 uL	250 μM
10 μMGAPDH primer, reverse	0.25 uL	250 μM
Nuclease-free Water	4.5 μL	-
Total	10 μL	-

Table S-T5: Reaction components for qPCR experiments described in **Fig. 6** and **Fig. S11.**

Table S-T6:

Cytometer Parameter	Aria II (BD)	SH800 (Sony)
Laser Interrogation Vessel	Rectangular Cuvette	Microfluidic Chip
Emission Optic Coupling	Gel-coupled	Air
Laser Excitation	Spatially Separate	Colinear
Laser Power	50 - 200 mW	30 mW
Acoustic Mechanism	Up-down	Side-side
Nozzle	Ring	Chip Integrated
ND Attenuation	Yes	No
Ease-of-Use	Requires expert training	Simple

Table S-T6: Comparison of FACS sorter instruments used in this work.